Proceeding of the IEEE
International Conference on Robotics and Biomimetics
Dali, China, December 2019

Dynamic Analysis and Control Design for a Tiltable Quadrotor

Hao Xu, Zhong Yang, Kaiwen Lu, Changliang Xu and Luwei Liao
College of Automation Engineering
Nanjing University of Aeronautics and Astronautics
Nanjing, Jiangsu Province, China
{ahaxuo, YangZhong, xuchangliang }@nuaa.edu.cn, {lkw_nuaa, liaoluweillw}@163.com

Qiuyan Zhang
Guizhou Electric Power Research Institute
Guizhou Power Grid Co., Ltd
Guiyang, Guizhou Province, China
zhangqycsg@163.com

Xiangrong Xu
School of Mechanical Engineering
Anhui University of Technology
Ma'anshan,Anhui Province ,China
xuxr@ahut.edu.cn

***Abstract*—This paper presents a tiltable quadrotor that can independently control position and attitude. Firstly, the dynamic modeling of the system is carried out. We adopted a nonlinear separation strategy for the nonlinear strong input problem existing in the system. We separated the nonlinear system into a linear dynamic link and a nonlinear static link by constructing an intermediate control quantity. Then, linear quadratic regulator with small calculation and easy hardware implementation was designed only for a linear dynamic link while real control, including tilting angle and motor speed, was mapped from intermediate control by calculating the input nonlinear static link. The simulation shows that the designed nonlinear controller based on nonlinear separation and LQR can stably control the tilting quadrotor and can independently track the position and attitude expectations.**

***Index Terms* - tiltable quadrotor, nonlinear separation, linear dynamic, LQR**

I. INTRODUCTION

Due to the simple mechanical structure, small size, lightweight, and high stability, multi-rotor aircraft has a wide range of applications in military and civilian fields, and related research continues to develop[1]. Multi-rotor aircraft have successfully applied in aerial photography, mapping, plant protection, and indoor navigation. Also, new applications—aerial manipulations [2-3] expanded. Aerial manipulations refer to the physical contact between the drone and the environment, including the capture of aerial or ground targets[4], the collection of tree specimens[5], and the installation of sensors[5]. The new application scenarios have also driven innovations in the mechanical structure and drive of drones, with many new configurations such as ducted drones[7], tilting fixed-wing aircraft[8], and tiltable multi-rotor drones[9].

The tiltable quadrotor UAV studied in this paper is one of the above new configurations. The difference from the conventional four-rotor is that its four rotors can rotate relative to the fuselage around the arm axis, turning the underactuated system into overdrive. A conventional four-rotor can only produce four independent outputs at the same time, including position and yaw angle or attitude and height, while the tiltable four-rotor can achieve full independent control of position and attitude, and the rotor tilt can form forces and torques in any direction[10]. However, the addition of the tilting rotor makes the tiltable quadrotor system more nonlinear and more coupled, which makes the design of the controller more difficult[11].

To the best of our knowledge, there are two types of solutions to the nonlinear problem of multi-rotor aircraft. One is to linearize the model and then design the controller, such as linearization at equilibrium[12] and feedback linearization[13]. The other is to design controllers directly for nonlinear models, such as nonlinear predictive control[14]. However, the input to the tiltable quadrotor system is non-linear, challenging to linearize at the equilibrium point and linearize the feedback. At the same time, the nonlinear predictive control method has the characteristics of vast computational complexity and difficult hardware implementation[15]. In this paper, we separated the tilting quadrotor system into a linear dynamic link and a nonlinear static link by constructing an intermediate control amount. Design a Linear Quadratic Regulator (LQR) for the separated linear dynamic link, and assign the central control amount to the actual control input by solving the nonlinear static link. The input is the rotor tilt angle and the motor speed. Finally, the simulation verifies the effectiveness and control effect of the designed controller.

II. MODELING OF THE SYSTEM

A. Coordinate system and symbol

As shown in Fig.1, the tiltable quadrotor studied can be viewed as five rigid body components, including the fuselage and four tilting rotor assemblies. Each tilting rotor assembly consists of steering gear and a motor, and the steering gear fixed by the motor controls the rotation of the body.

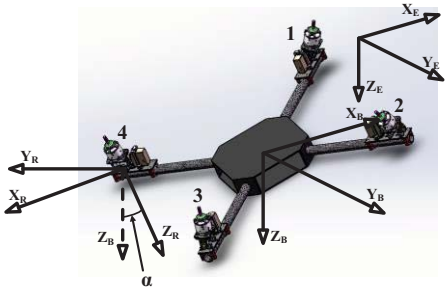

Fig.1 Frames of the quadrotor with tiltable-rotors

The inertial coordinate system fixed to the ground is defined as $\mathcal{F}_E$:$\{O_E;\ X_E,\ Y_E,\ Z_E\}$ z-axis points downward, and the x axis points north; The body coordinate system fixed at the centroid of the tiltable quadrotor is defined as $\mathcal{F}_B$:$\{O_B;\ X_B,\ Y_B,\ Z_B\}$ the z-axis is also pointing downwards, and the x-axis is pointing to the front of the body. Also defined $\mathcal{F}_{R_i}$:$\{O_{R_i};\ X_{R_i},\ Y_{R_i},\ Z_{R_i}\}$ as the i-th rotor coordinate system， the origin is fixed to the center of mass of

[1]* This work is partially supported by the National Natural Science Foundation of China under Grant 61473144,in part by in part by the Key Laboratory Projects of Aeronautical Science Foundation of China under Grant 20162852031, in part by the Science and Technology Projects of China Southern Power Grid Co. Ltd. under Grant 066600KK52170074, in part by the National Key R&D Plan under Grant 2017YFE0113200.

978-1-7281-6321-5/19//$31.00 ©2019 IEEE

the tilting rotor assembly. The x-axis pointed the centroid of the machine to the centroid of the rotor assembly. The rotor coordinate system $\mathcal{F}_{R_i}$ rotated around the x-axis with a rotation angle of α_i

The symbols used in this article follow the rules below. The upper right mark indicates the coordinate system in which the reference symbol located. For example, $\boldsymbol{P}^E$ is the position description of the centroid of the aircraft in the inertial coordinate system. ${}^{(\cdot)}\boldsymbol{R}_{(\cdot)} \in SO(3)$ is the rotation matrix between different coordinate systems, $\mathrm{s}_{(\cdot)}, \mathrm{c}_{(\cdot)}, \mathrm{t}_{(\cdot)}$ are abbreviations for $\sin(\cdot), \cos(\cdot), \tan(\cdot)$, $\boldsymbol{R}_X(\cdot), \boldsymbol{R}_Y(\cdot), \boldsymbol{R}_Z(\cdot)$ are rotations about three axes.

$$\begin{aligned}
\boldsymbol{R}_X(\cdot) &= \begin{pmatrix} 1 & 0 & 0 \\ 0 & \cos(\cdot) & -\sin(\cdot) \\ 0 & \sin(\cdot) & \cos(\cdot) \end{pmatrix} \\
\boldsymbol{R}_Y(\cdot) &= \begin{pmatrix} \cos(\cdot) & 0 & \sin(\cdot) \\ 0 & 1 & 0 \\ -\sin(\cdot) & 0 & \cos(\cdot) \end{pmatrix} \\
\boldsymbol{R}_Z(\cdot) &= \begin{pmatrix} \cos(\cdot) & -\sin(\cdot) & 0 \\ \sin(\cdot) & \cos(\cdot) & 0 \\ 0 & 0 & 1 \end{pmatrix}
\end{aligned} \tag{1}$$

In this paper, the Euler angle adopts the Z-Y-X sequence, so the rotation matrix of the body coordinate system to the inertial system is

$${}^E\boldsymbol{R}_B = \boldsymbol{R}_Z(\psi)\boldsymbol{R}_Y(\theta)\boldsymbol{R}_X(\phi) \tag{2}$$

${}^B\boldsymbol{R}_{R_i}$ represents the rotation matrix from the rotor coordinate system to the body coordinate system

$${}^B\boldsymbol{R}_{R_i} == \boldsymbol{R}_Z((i-1)\frac{\pi}{2})\boldsymbol{R}_X(\alpha_i) \tag{3}$$

The origin $\boldsymbol{O}_{R_i}$ of the rotor coordinate system in the machine system is

$$\boldsymbol{O}_{R_i}^B = \boldsymbol{R}_Z\left((i-1)\frac{\pi}{2}\right)\begin{bmatrix} 0 \\ 0 \\ l \end{bmatrix}, \qquad i = 1...4 \tag{4}$$

B. Dynamic modeling

The tilting position of the tilting aircraft studied in this paper is at the centroid position. The moving speed of the inertial coordinate system is $\boldsymbol{P}^E = \begin{bmatrix} x & y & z \end{bmatrix}^{\mathrm{T}}$ and $\boldsymbol{V}^E = \begin{bmatrix} u & v & w \end{bmatrix}^{\mathrm{T}}$ respectively.The Euler angle of the craft is $\boldsymbol{\Theta} = \begin{bmatrix} \phi & \theta & \psi \end{bmatrix}^{\mathrm{T}}$. The angular velocity of the body under the machine system is $\boldsymbol{\Omega}^B = \begin{bmatrix} p & q & r \end{bmatrix}^{\mathrm{T}}$, and

$$\dot{\boldsymbol{\Theta}} = \begin{bmatrix} 1 & \mathrm{t}_\theta \mathrm{s}_\phi & \mathrm{t}_\theta \mathrm{c}_\phi \\ 0 & \mathrm{c}_\phi & -\mathrm{s}_\phi \\ 0 & \mathrm{s}_\phi / \mathrm{c}_\theta & \mathrm{c}_\phi / \mathrm{c}_\theta \end{bmatrix} \dot{\boldsymbol{\Omega}}^B \tag{5}$$

At the equilibrium point, when $\boldsymbol{\Theta} = \begin{bmatrix} 0 & 0 & 0 \end{bmatrix}^{\mathrm{T}}$, there is $\dot{\boldsymbol{\Theta}} = \dot{\boldsymbol{\Omega}}^B$.

To establish a dynamic model, make the following assumptions. Both the aircraft body and the tilting rotor assembly are rigid and inelastically deformed; Each rotor rotation axis passes through the rotor, motor and steering gear centroid;In the absence of wind, the lift, and counter-torque generated by the rotor are proportional to the square of the rotor speed; Euler angle, translational speed, and angular velocity are small during the movement of the body; The dynamic process of the steering gear is independent of the rotor speed.

We established the rigid body dynamics model by the Newton-Eulerian equation [16]. We described the translation in the inertial coordinate system and described the rotational equation in the machine system.

$$\begin{bmatrix} m\dot{\boldsymbol{V}}^E \\ \boldsymbol{I}_B\dot{\boldsymbol{\Omega}}^B \end{bmatrix} + \begin{bmatrix} \boldsymbol{0} \\ \boldsymbol{\Omega}^B \times (\boldsymbol{I}_B\boldsymbol{\Omega}^B) \end{bmatrix} = \begin{bmatrix} \boldsymbol{F}_{ext}^E \\ \boldsymbol{M}_{ext}^B \end{bmatrix} \tag{6}$$

Where m is the total mass of the aircraft system, $\boldsymbol{I}_B = \mathrm{diag}(I_{xx}, I_{yy}, I_{zz})$ is the inertia matrix of the aircraft.

Ignore the air resistance and analyze the force of the aircraft. The external system force is composed of gravity $\boldsymbol{F}_g^E$ and the thrust $\boldsymbol{F}_t^E$ generated by the rotor.

$$\begin{aligned}
&\boldsymbol{F}_{ext}^E = m\begin{bmatrix} 0 \\ 0 \\ g \end{bmatrix} + {}^E\boldsymbol{R}_B\sum_{i=1}^{4}{}^B\boldsymbol{R}_{R_i}\boldsymbol{T}_i, \quad \boldsymbol{T}_i = \begin{bmatrix} 0 \\ 0 \\ T_i \end{bmatrix} \\
&T_i = \text{-}k_f n_i^2, \qquad k_f > 0,
\end{aligned} \tag{7}$$

Where k_f is the rotor thrust coefficient, n_i is the speed of the $i-th$ rotor

The external torque consists of four parts, including the moment $\boldsymbol{M}_t$ generated by the rotor thrust, the rotor rotation counter-torque $\boldsymbol{M}_{anti}$, the steering gear counter-torque $\boldsymbol{M}_{\alpha,\beta}$, and the gyro effect term $\boldsymbol{M}_{gyro}$.

$$\boldsymbol{M}^B = \boldsymbol{M}_t^B + \boldsymbol{M}_{anti}^B + \boldsymbol{M}_\alpha^B + \boldsymbol{M}_{gyro}^B, \tag{8}$$

The torque generated by the rotor thrust under the machine system is.

$$\boldsymbol{M}_t^B = \sum_{i=1}^{4}\left(\boldsymbol{O}_{R_i}^B \times {}^B\boldsymbol{R}_{R_i}\boldsymbol{T}_i\right). \tag{9}$$

The rotor 1 rotates clockwise, the rotor 2 rotates counterclockwise, and the counter-torque torque formed by the rotation of the rotor is $\boldsymbol{Q}_i$ under the rotor coordinate system.

$$\begin{aligned}
&\boldsymbol{M}_{anti}^B = \sum_{i=1}^{4}\left({}^B\boldsymbol{R}_{R_i}\boldsymbol{Q}_i\right), \\
&\boldsymbol{Q}_i = [0 \quad 0 \quad Q_i]^T, \\
&Q_i = (\text{-}1)^{i-1}k_m n_i^2, \qquad k_m > 0.
\end{aligned} \tag{10}$$

We correlated Rudder reverse torque with tilt angular acceleration negatively.

$$\boldsymbol{M}_\alpha^B = \sum_{i=1}^{4}\left({}^B\boldsymbol{R}_{R_i}\begin{bmatrix} \text{-}J_\alpha\ddot{\alpha}_i \\ 0 \\ 0 \end{bmatrix}\right) \tag{11}$$

We calculated the gyroscopic effect torque according to the angular velocity of the motor and the rotational speed of the rotor.

$$\boldsymbol{M}_{gyro}^{B} = J_p \sum_{i=1}^{4} \left(\left(\boldsymbol{\Omega}^{B} + {}^{B}\boldsymbol{R}_{P_i} \begin{bmatrix} \dot{\alpha}_i \\ 0 \\ 0 \end{bmatrix} \right) \times (-1)^{f(i)} {}^{B}\boldsymbol{R}_{P_i} \begin{bmatrix} 0 \\ 0 \\ n_i \end{bmatrix} \right), \quad (12)$$

$$f(i) = \begin{cases} 0, & i = 1,2 \\ 1. & i = 3,4 \end{cases}.$$

Combined (6) to (12), the tiltable quadrotor dynamical model is

$$\begin{aligned} \dot{u} = \frac{1}{m} \{ & \left(\mathrm{s}_{\phi}\mathrm{s}_{\varphi} + \mathrm{c}_{\phi}\mathrm{c}_{\varphi}\mathrm{s}_{\theta} \right)(T_1 \mathrm{c}_{\alpha_1} + T_2 \mathrm{c}_{\alpha_2} + T_3 \mathrm{c}_{\alpha_3} + T_4 \mathrm{c}_{\alpha_4}) \\ & + \left(\mathrm{c}_{\phi}\mathrm{s}_{\varphi} - \mathrm{c}_{\varphi}\mathrm{s}_{\phi}\mathrm{s}_{\theta} \right)\left(T_1 \mathrm{s}_{\alpha_1} - T_3 \mathrm{s}_{\alpha_3} \right) \\ & + \mathrm{c}_{\varphi}\mathrm{c}_{\theta}\left(T_2 \mathrm{s}_{\alpha_2} - T_4 \mathrm{s}_{\alpha_4} \right) \} \end{aligned} \quad (13)$$

$$\begin{aligned} \dot{v} = \frac{1}{m} \{ & -\left(\mathrm{c}_{\varphi}\mathrm{s}_{\phi} - \mathrm{c}_{\phi}\mathrm{s}_{\varphi}\mathrm{s}_{\theta} \right)(T_1 \mathrm{c}_{\alpha_1} + T_2 \mathrm{c}_{\alpha_2} + T_3 \mathrm{c}_{\alpha_3} + T_4 \mathrm{c}_{\alpha_4}) \\ & - \left(\mathrm{c}_{\phi}\mathrm{c}_{\varphi} + \mathrm{s}_{\varphi}\mathrm{s}_{\phi}\mathrm{s}_{\theta} \right)\left(T_1 \mathrm{s}_{\alpha_1} - T_3 \mathrm{s}_{\alpha_3} \right) \\ & + \mathrm{c}_{\theta}\mathrm{s}_{\varphi}\left(T_2 \mathrm{s}_{\alpha_2} - T_4 \mathrm{s}_{\alpha_4} \right) \} \end{aligned} \quad (14)$$

$$\begin{aligned} \dot{w} = g + \frac{1}{m} \{ & \mathrm{c}_{\phi}\mathrm{c}_{\theta}(T_1 \mathrm{c}_{\alpha_1} + \mathrm{T}_2\mathrm{c}_{\alpha_2} + \mathrm{T}_3\mathrm{c}_{\alpha_3} + \mathrm{T}_4\mathrm{c}_{\alpha_4}) \\ & - \mathrm{c}_{\theta}\mathrm{s}_{\phi}\left(T_1 \mathrm{s}_{\alpha_1} - \mathrm{T}_3 \mathrm{s}_{\alpha_3} \right) - \mathrm{s}_{\theta}\left(T_2 \mathrm{s}_{\alpha_2} - T_4 \mathrm{s}_{\alpha_4} \right) \} \end{aligned} \quad (15)$$

$$\begin{aligned} \dot{p} = \frac{1}{I_{xx}} \{ & (I_{yy} - I_{zz})qr + l(T_2 \mathrm{c}_{\alpha_2} - T_4 \mathrm{c}_{\alpha_4}) \\ & + Q_2 \mathrm{s}_{\alpha_2} - Q_4 \mathrm{s}_{\alpha_4} + J_{\alpha}(\ddot{\alpha}_3 - \ddot{\alpha}_1) \\ & + \mathrm{J}_p [q(n_1 \mathrm{c}_{\alpha_1} - n_3 \mathrm{c}_{\alpha_3}) + r(n_1 \mathrm{s}_{\alpha_1} + n_3 \mathrm{s}_{\alpha_3}) \\ & + \omega_2 \mathrm{c}_{\alpha_2}(\dot{\alpha}_2 + q) + \omega_4 \mathrm{c}_{\alpha_4}(\dot{\alpha}_4 - q)] \} \end{aligned} \quad (16)$$

$$\begin{aligned} \dot{q} = \frac{1}{I_{yy}} \{ & \left(I_{zz} - I_{xx} \right) pr + l(-T_1 \mathrm{c}_{\alpha_1} + T_3 \mathrm{c}_{\alpha_3}) \\ & - Q_1 \mathrm{s}_{\alpha_1} + Q_3 \mathrm{s}_{\alpha_3} + J_{\alpha}(\ddot{\alpha}_4 - \ddot{\alpha}_2) \\ & + \mathrm{J}_p [p(n_4 \mathrm{c}_{\alpha_4} - n_2 \mathrm{c}_{\alpha_2}) + r(n_2 \mathrm{s}_{\alpha_2} + \omega_4 \mathrm{s}_{\alpha_4}) \\ & - n_1 \mathrm{c}_{\alpha_1}(\dot{\alpha}_1 + p) - n_3 \mathrm{c}_{\alpha_3}(\dot{\alpha}_3 - p)] \} \end{aligned} \quad (17)$$

$$\begin{aligned} \dot{r} = \frac{1}{I_{zz}} \{ & \left(I_{xx} - I_{yy} \right) pq + l(-T_1 \mathrm{s}_{\alpha_1} - T_2 \mathrm{s}_{\alpha_2} - T_3 \mathrm{s}_{\alpha_3} - T_4 \mathrm{s}_{\alpha_4}) \\ & + Q_1 \mathrm{c}_{\alpha_1} + Q_2 \mathrm{c}_{\alpha_2} + Q_3 \mathrm{c}_{\alpha_3} + Q_4 \mathrm{c}_{\alpha_4} \\ & + J_p [-n_1 \mathrm{s}_{\alpha_1}(\dot{\alpha}_1 + p) - n_2 \mathrm{s}_{\alpha_2}(\dot{\alpha}_2 + q) \\ & + n_3 \mathrm{s}_{\alpha_3}(\dot{\alpha}_3 - p) + n_4 \mathrm{s}_{\alpha_4}(\dot{\alpha}_4 - q)] \} \end{aligned} \quad (18)$$

III. CONTROLLER DESIGN

A. System nonlinear separation

The conventional four-rotor system has only four control inputs, namely four-rotor speeds n_i, so it can only track four independent outputs, so the researchers now divide the flight control of the four-rotor into position mode and attitude mode. Position mode tracking position and yaw angle, attitude mode tracking attitude angle and height[17]. The tiltable quadrotor system has eight control inputs, including four-rotor speeds n_i and four-rotor tilt angles α_i, which are input redundancy systems. Through the tilting of the four rotors, we formed the control force and control torque in any direction and tracked the position expectation and attitude expectation at the same time.

However, while the rotor tilting changes the thrust direction, the coupling and nonlinearity of the system are greatly enhanced, and controller design is more complicated. Therefore, it is necessary to simplify the decoupling and linearization of the system dynamics model represented by (13-18) to make it easy to design the controller.

First, we ignored the gyro effect and the tilting counter-torque inside the system in the simplified model as a second-order disturbance term. The simplified dynamic model is

$$\begin{cases} \ddot{\boldsymbol{P}}^{E} = \begin{bmatrix} 0 \\ 0 \\ g \end{bmatrix} + \frac{1}{m} {}^{E}\boldsymbol{R}_{B} \sum_{i=1}^{4} {}^{B}\boldsymbol{R}_{R_i} \boldsymbol{T}_i \\ \ddot{\boldsymbol{\Theta}} = \boldsymbol{I}_{B}^{-1} \left(\sum_{i=1}^{4} \left(\boldsymbol{O}_{R_i}^{B} \times {}^{B}\boldsymbol{R}_{R_i} \boldsymbol{T}_i \right) + \sum_{i=1}^{4} \left({}^{B}\boldsymbol{R}_{R_i} \boldsymbol{Q}_i \right) \right) \end{cases}. \quad (19)$$

Secondly, we assumed that the fast high gain controller is used to track the desired rotation angle α_i and the speed n_i inside the steering gear and the motor that the dynamic process of the steering gear and the motor can be ignored. Considering (14) is mainly a nonlinear input, the system can be decomposed into linear dynamic links and nonlinear static links by constructing intermediate control quantities $\boldsymbol{U}_F^E = \begin{bmatrix} F_x & F_y & F_z \end{bmatrix}^{\mathrm{T}}$ and $\boldsymbol{U}_M^E = \begin{bmatrix} M_x & M_y & M_z \end{bmatrix}^{\mathrm{T}}$. For the design of dynamic link, the intermediate control quantity outputted by the controller is mapped to the motor speed n_i and the steering angle α_i through the nonlinear static link.

The linear dynamic link is as follows

$$\begin{cases} \dot{\boldsymbol{V}}^{E} = \begin{bmatrix} 0 \\ 0 \\ g \end{bmatrix} + \frac{1}{m} \boldsymbol{U}_F^E \\ \dot{\boldsymbol{\Omega}}^{B} = \boldsymbol{I}_{B}^{-1} \boldsymbol{U}_M^E \end{cases} \quad (20)$$

The nonlinear static link is as follows

$$\begin{bmatrix} \left({}^{E}\boldsymbol{R}_{B} \right)^{\mathrm{T}} \boldsymbol{U}_F^E \\ \boldsymbol{U}_M^B \end{bmatrix} = \boldsymbol{A}(\alpha) \begin{bmatrix} n_1^2 \\ n_2^2 \\ n_3^2 \\ n_4^2 \end{bmatrix} \quad (21)$$

In the controller design, the mapping from the standard control to the motor speed and the steering angle is called control distribution and $A(\alpha)$ is the control distribution matrix. For a conventional quadrotor, the control distribution matrix is constant, but in the tiltable quadrotor studied in this paper, it is a α function. For the problem of nonlinear control allocation, the researchers proposed nonlinear programming method, dynamic optimization method, etc. [18], but these methods require more computing time and computing resources. In [15], it proposed a method for constructing a virtual quantity linearized control distribution matrix for the tilting rotor. We extended this method to a tiltable quadrotor in the paper.

Introducing $N_{l,i} = n_i^2 s_{\alpha_i}$, $N_{v,i} = n_i^2 c_{\alpha_i}$ in (21), there is

$$\begin{bmatrix} \left({}^{E}\boldsymbol{R}_{B}\right)^{\mathrm{T}}\boldsymbol{U}_{F}^{E} \\ \boldsymbol{U}_{M}^{B} \end{bmatrix} = \boldsymbol{A}\boldsymbol{N}, \qquad (22)$$

$$\boldsymbol{N} = \left[N_{l,1}, N_{v,1}, \ldots N_{l,4}, N_{v,4}\right]^{\mathrm{T}}$$

The control distribution matrix $\boldsymbol{A}$ in (22) is a constant matrix, independent of the tilt angle. And $\boldsymbol{A}$ is a row full rank matrix, and the virtual amount $\boldsymbol{N}$ can be calculated by finding the Moore-Penrose pseudoinverse of $\boldsymbol{A}$

$$\boldsymbol{N} = \boldsymbol{A}^{+}\begin{bmatrix} \left({}^{E}\boldsymbol{R}_{B}\right)^{T}\boldsymbol{U}_{F}^{E} \\ \boldsymbol{U}_{M}^{B} \end{bmatrix} \qquad (23)$$

Then directly calculate the rotor speed and tilt angle

$$\begin{aligned} n_i^2 &= \sqrt{(N_{v,i}^2 + N_{l,i}^2)} \\ \alpha_i &= \operatorname{atan2}(N_{l,i}, N_{v,i}) \end{aligned} \qquad (24)$$

B. *LQR pose design*

The linear quadratic regulator is a kind of optimal regulator with widely application. Its performance index is the quadratic function of the object state and control input. The optimal solution has a unified analytical expression, which is easy to find the optimal solution and easy to implement in engineering.By analyzing the linear dynamic process corresponding to (20), we found that the dynamic process of position and attitude is decoupled, so the position controller and attitude controller are designed separately.

Assuming that the quadrotor is stable in a specific set state, the given position expects $\boldsymbol{P}_d^E = \begin{bmatrix} x_d & y_d & z_d \end{bmatrix}^{\mathrm{T}}$, the expected input $(\boldsymbol{U}_F^E)_d = \begin{bmatrix} 0 & 0 & mg \end{bmatrix}^{\mathrm{T}}$, and defines the following state quantity, input quantity, and output quantity,

$$\begin{cases} \boldsymbol{X}_p(t) = \begin{bmatrix} x - x_d & (x - x_d)' & y - y_d & (y - y_d)' & z - z_d & (z - z_d)' \end{bmatrix}^{\mathrm{T}} \\ \Delta\boldsymbol{U}_F^E(t) = \boldsymbol{U}_F^E - (\boldsymbol{U}_F^E)_d = \begin{bmatrix} F_x & F_y & F_z - mg \end{bmatrix}^{\mathrm{T}} \\ \Delta\boldsymbol{P}^E(t) = \begin{bmatrix} x - x_d & y - y_d & z - z_d \end{bmatrix}^{\mathrm{T}} \end{cases} \qquad (25)$$

We described the state-space of the position control model as

$$\begin{cases} \dot{\boldsymbol{X}}_p(t) = \boldsymbol{A}_p\boldsymbol{X}_p(t) + \boldsymbol{B}_p\Delta\boldsymbol{U}_F^E(t) \\ \Delta\boldsymbol{P}(t) = \boldsymbol{C}_p\boldsymbol{X}_p(t) \end{cases} \qquad (26)$$

$$\boldsymbol{A}_p = \begin{bmatrix} 0 & 1 & 0 & 0 & 0 & 0 \\ 0 & 0 & 0 & 0 & 0 & 0 \\ 0 & 0 & 0 & 1 & 0 & 0 \\ 0 & 0 & 0 & 0 & 0 & 0 \\ 0 & 0 & 0 & 0 & 0 & 1 \\ 0 & 0 & 0 & 0 & 0 & 0 \end{bmatrix}, \boldsymbol{B}_p = \begin{bmatrix} 0 & 0 & 0 \\ 1/m & 0 & 0 \\ 0 & 0 & 0 \\ 0 & 1/m & 0 \\ 0 & 0 & 0 \\ 0 & 0 & 1/m \end{bmatrix} \qquad (27)$$

With the similar representation, we give the posture expectation $\boldsymbol{\Theta}_d = \begin{bmatrix} \phi_d & \theta_d & \psi_d \end{bmatrix}^{\mathrm{T}}$ and expected input $(\boldsymbol{U}_M^B)_d = \boldsymbol{O}_{3\times1}$, the following state quantities, input quantities, and outputs are defined.

$$\begin{cases} \boldsymbol{X}_\Theta(t) = \begin{bmatrix} \phi - \phi_d & (\phi - \phi_d)' & \theta - \theta_d & (\theta - \theta_d)' & \psi - \psi_d & (\psi - \psi_d)' \end{bmatrix}^{\mathrm{T}} \\ \Delta\boldsymbol{U}_M^B(t) = \boldsymbol{U}_M^B - (\boldsymbol{U}_M^B)_d = \begin{bmatrix} M_x & M_y & M_z \end{bmatrix}^{\mathrm{T}} \\ \Delta\boldsymbol{\Theta}(t) = \begin{bmatrix} \phi - \phi_d & \theta - \theta_d & \psi - \psi_d \end{bmatrix}^{\mathrm{T}} \end{cases} \qquad (28)$$

We described the state-space of the position control model as

$$\begin{cases} \dot{\boldsymbol{X}}_\Theta(t) = \boldsymbol{A}_\Theta\boldsymbol{X}_\Theta(t) + \boldsymbol{B}_\Theta\Delta\boldsymbol{U}_M^B(t) \\ \Delta\boldsymbol{\Theta}(t) = \boldsymbol{C}_\Theta\boldsymbol{X}_\Theta(t) \end{cases} \qquad (29)$$

$$\boldsymbol{A}_\Theta = \begin{bmatrix} 0 & 1 & 0 & 0 & 0 & 0 \\ 0 & 0 & 0 & 0 & 0 & 0 \\ 0 & 0 & 0 & 1 & 0 & 0 \\ 0 & 0 & 0 & 0 & 0 & 0 \\ 0 & 0 & 0 & 0 & 0 & 1 \\ 0 & 0 & 0 & 0 & 0 & 0 \end{bmatrix}, \boldsymbol{B}_\Theta = \begin{bmatrix} 0 & 0 & 0 \\ 1/I_{xx} & 0 & 0 \\ 0 & 0 & 0 \\ 0 & 1/I_{yy} & 0 \\ 0 & 0 & 0 \\ 0 & 0 & 1/I_{zz} \end{bmatrix} \qquad (30)$$

C. *Optimal control law*

The performance metric for defining LQR is

$$J = \frac{1}{2}\int\left[\boldsymbol{X}^{\mathrm{T}}(t)\boldsymbol{Q}\boldsymbol{X}(t) + \Delta\boldsymbol{U}^{\mathrm{T}}(t)\boldsymbol{R}\Delta\boldsymbol{U}(t)\right]\mathrm{d}t \qquad (31)$$

Where $\boldsymbol{Q}$ is the weighting matrix of the state variable, which is a real symmetric semi-definite matrix, and $\boldsymbol{R}$ is the weighting matrix of the input quantity, which is a real symmetric positive definite matrix. Solving quadratic optimal control is to find the state feedback control law $\Delta\boldsymbol{U}(t)$ so that J takes a minimum value. The most common solution is to use the Ricatti equation.

$$\dot{\boldsymbol{K}} + \boldsymbol{Q} - \boldsymbol{K}^{\mathrm{T}}\boldsymbol{B}\boldsymbol{R}^{-1}\boldsymbol{B}^{\mathrm{T}}\boldsymbol{K}^{\mathrm{T}} + \boldsymbol{K}\boldsymbol{A} + \boldsymbol{A}^{\mathrm{T}}\boldsymbol{K}^{\mathrm{T}} = 0 \qquad (32)$$

LQR optimal control law is

$$\begin{cases} \Delta\boldsymbol{U}(t) = -\boldsymbol{R}^{-1}\boldsymbol{B}^{T}\boldsymbol{K}\boldsymbol{X}(t) \\ \boldsymbol{U}(t) = \boldsymbol{U}_d + \Delta\boldsymbol{U}(t) \end{cases} \qquad (33)$$

After many attempts, we obtained the position controller $\boldsymbol{Q}$ and the attitude controller $\boldsymbol{R}$ which make the system perform well.

$$\begin{aligned} \boldsymbol{Q}_P &= diag(81.7,12.4,81.7,12.4,81.7,12.4) \\ \boldsymbol{R}_P &= diag(1,1,1) \\ \boldsymbol{Q}_\Theta &= diag(15,2.8,15,2.8,15,2.8) \\ \boldsymbol{R}_\Theta &= diag(1,1,1) \end{aligned} \qquad (34)$$

IV. SIMULATION

Set up the simulation environment in MATLAB (see Fig.2) to verify the performance of the designed position and attitude controller. Table 1 shows the physical parameters of the tiltable quadrotor.

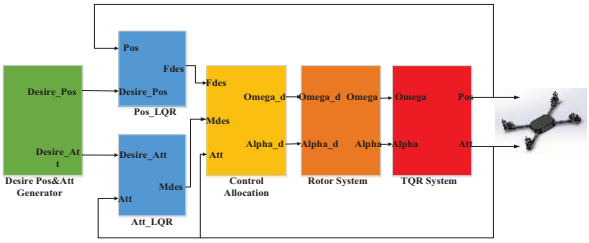

Fig2. Structure diagram of linear quadratic regulator simulation

Table 1 Physic parameters of System

Symbol	Physical meaning	Value
m	Quality	$1.38kg$
g	Gravity	$9.81\,m\cdot s^{-2}$
I_{xx} / I_{yy}	X-axis/Y-axis inertia tensor	$0.0298\,kg\cdot m^2$
I_{zz}	Z-axis inertia tensor	$0.571\,kg\cdot m^2$
k_f	Lift coefficient	$3.10e-5$
k_m	Resistance coefficient	$5.61e-7$
J_α	Moment of inertia on tilting shaft	$1.50e-5\,kg\cdot m^2$
J_p	Gyro moment coefficient	$6.00e-5$

A. Stability control simulation

First, verify the stability control effect of the LQR controller on the tiltable quadrotor. Set the initial position of the aircraft to $\boldsymbol{P}_0^E = [0 \quad 0 \quad 0]^{\mathrm{T}}$ (m) the initial attitude to $\boldsymbol{\Theta}_0 = [0 \quad 0 \quad 0]^{\mathrm{T}}$ (°) and the control target is $\boldsymbol{P}_d^E = [3 \quad 4 \quad -2]^{\mathrm{T}}$ (m) $\boldsymbol{\Theta}_d = [15 \quad 30 \quad 25]^{\mathrm{T}}$ (°). Fig.3 shows the simulation results.

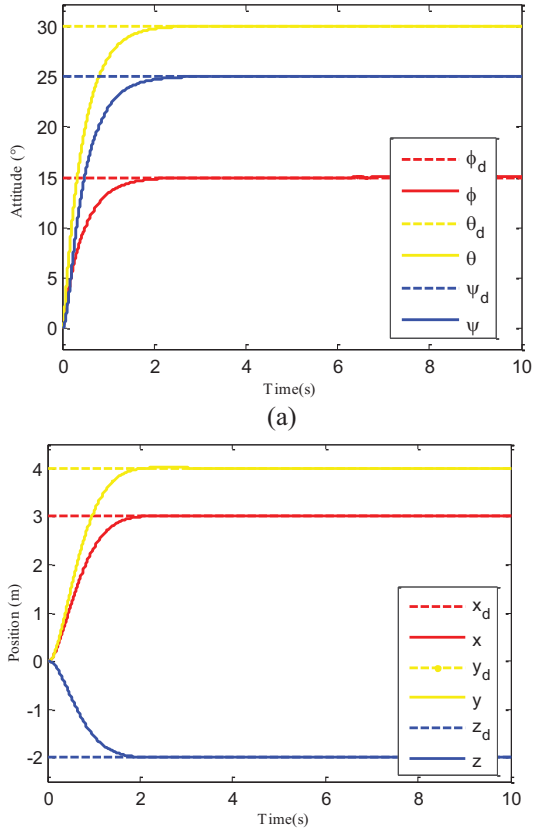

Fig.3 Response curves of position and attitude in stability experiment

Fig. 3 shows that the position and attitude angles are very smooth and reach the desired value. There is no oscillation during the adjustment process, and almost no overshoot. It can be seen that the LQR controller is ideal for the stable control of the quadrotor. It can reach the target position and reach the target attitude in about 2s, and hovering at the target position.

Conventional quadrotors can only hover without roll and pitchless. When there is a roll angle or pitch angle, the thrust force of the rotors produces a component in the horizontal direction, causing the rotor to move horizontally. The tiltable quadrotor can hover at non-zero roll angles and non-zero attitude angles, thanks to the tilting of the rotor to create control and control torque in any direction. Even if there is a roll angle and a pitch angle, the rotor thrust force can be controlled to be vertically upward and balanced with gravity.

A. Independent position and attitude tracking

Unlike conventional quadrotors, tiltable quadrotors enable independent control of position and attitude. In this paper, we designed the position tracking experiment of fixed attitude and the attitude tracking experiment of fixed point hover. These experiments verified the ability of the LQR controller to control the position and attitude of the tiltable quadrotor independently.

1)Set the initial state $\boldsymbol{P}_0^E = [0 \quad 0 \quad 0]^{\mathrm{T}}$ (m) and $\boldsymbol{\Theta}_0 = [0 \quad 0 \quad 0]^{\mathrm{T}}$ (°) of the aircraft, reach three meters in five seconds, and set $\phi = 10°, \theta = 5°$. In the fifth second, controller tracked the position expectation of (26). Fig. 4(a) shows the position feedback and Fig. 4(b) is the synchronized attitude response curve.

$$\boldsymbol{P}_d^E = \left[5\sin\left(\frac{\pi}{10}(t-5)\right) \quad 5\cos\left(\frac{\pi}{10}(t-5)\right)-5 \quad -\frac{3}{5}t \right]^{\mathrm{T}} \quad (26)$$

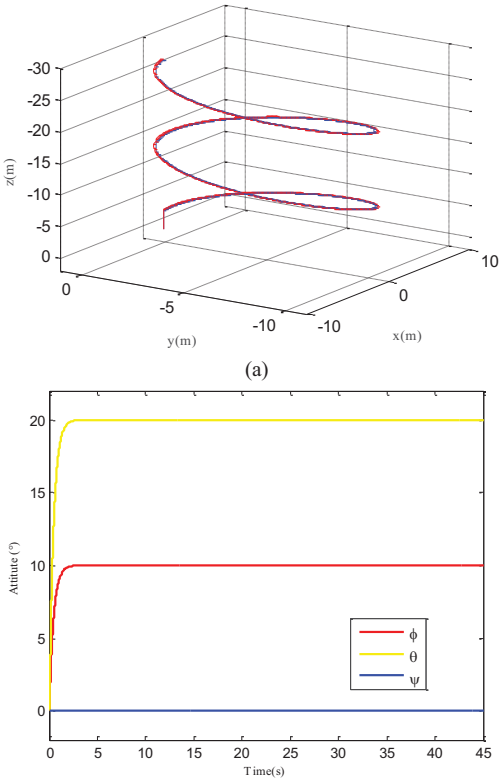

Fig.4 Response curves of position tracking under static attitude

2)Setting the initial state of the aircraft $\boldsymbol{P}_0^E = [0 \quad 0 \quad 0]^{\mathrm{T}}$ (m) and $\boldsymbol{\Theta}_0 = [0 \quad 0 \quad 0]^{\mathrm{T}}$ (°), track the square wave attitude expectation, and hover at the position $\boldsymbol{P}_d^E = [2 \quad 3 \quad -2]^{\mathrm{T}}$ (m). Fig. 5 shows the output curve of the system.

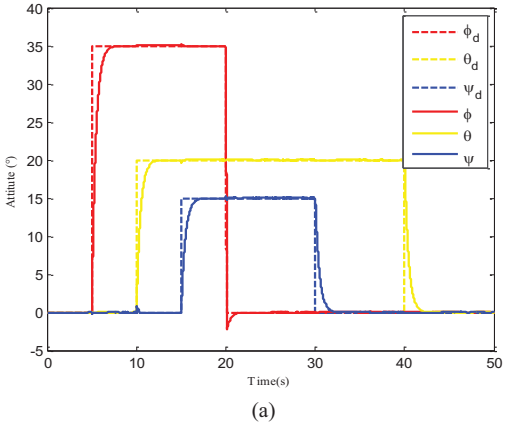

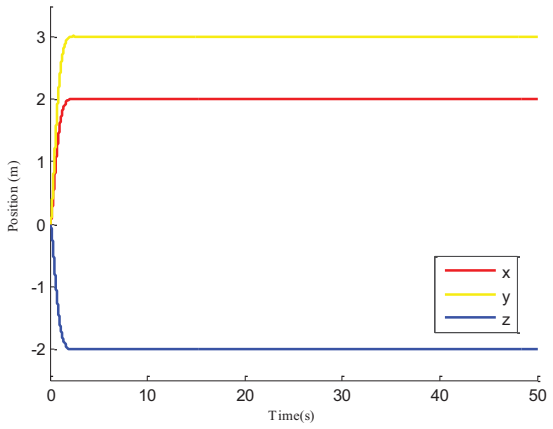

(b)

Fig.5 Response curves of attitude tracking without position change

From the experimental results shown in Fig. 4 and Fig. 5, the tilting quadrotor designed in this paper can track the positional expectation in the form of a trigonometric function and the attitude expectation in the form of square wave. The LQR controller tracks quickly and the control is stable. Also, the aircraft can maintain the attitude at a given attitude during position tracking. When hovering at a fixed point, the controller can still track the given pose. Therefore, the LQR controller can well control the position and attitude of the tiltable quadrotor.

V. CONCLUSION

We established a dynamic model with a tiltable quadrotor in this paper. Because of the strong nonlinearity and coupling of the system model, it is challenging to design controller problems. We construct the intermediate control quantity to separate the system into linear dynamic link and nonlinear static link and design the LQR optimal controller to control the linear dynamic link after separation. The controller maps the intermediate control amount to the actual control amount by solving the nonlinear static process. The simulation results show that the LQR controller based on the separated linear dynamic link design has a good effect on controlling the position and attitude of the tiltable aircraft.

REFERENCES

[1] Liu Yisha, YANG Shengxuan, WANG Wei, "An active disturbance rejection flight control method for quad-rotor unmanned aerial vehicles, *Control Theory & Applications*, vol. 32,no. 10, pp.1351-1360, 2015.

[2] KHAMSEH H B, JANABISHARIFI F, ABDESSAMEUD A, et al, "Aerial manipulation—A literature survey" . *Robotics and Autonomous Systems*, pp. 221-235, 2018.

[3]Yang Bin, He Yuqing, Han Jianda, et al, "Survey on aerial manipulator systems," *Robot* , vol. 37, no. 5, pp. 628-640, 2015.

[4] GAWEL A, KAMEL M, NOVKOVIC T, et al, "Aerial picking and delivery of magnetic objects with MAVs," *International Conference on Robotics and Automation*, pp. 5746-5752, 2017.

[5] Kutia J R, Stol K A, Xu W, et al, "Aerial Manipulator Interactions With Trees for Canopy Sampling" . *IEEE-ASME Transactions on Mechatronics*, vol. 23, no. 4, pp. 1740-1749, 2018.

[6] Orsag M, Korpela C M, Bogdan S, et al, "Hybrid adaptive control for aerial manipulation," *Journal of Intelligent & Robotic Systems* , vol. 73, no.1-4, pp. 693-707, 2014.

[7] Muehlebach M, Andrea R D, "The Flying Platform – A testbed for ducted fan actuation and control design," *Mechatronics*, pp. 52-68, 2017.

[8] Chowdhury A B , Kulhare A , Raina G , "Back-stepping Control Strategy for Stabilization of a Tilt-rotor UAV," *IEEE Control & Decision Conference*, 2012.

[9] RYLL M, BULTHOFF H H, GIORDANO P R, et al, "First flight tests for a quadrotor UAV with tilting propellers," *International Conference on Robotics and Automation*, pp. 295-302, 2013.

[10] RYLL M, Bulthoff H H, Giordano P R, et al, "Modeling and control of a quadrotor UAV with tilting propellers," *International Conference on Robotics and Automation*, pp. 4606-4613, 2012.

[11] SCHOLZ G, TROMMER G F, "Model Based Control of a Quadrotor with Tiltable Rotors," *Gyroscopy and Navigation*, vol. 7,no. 1, pp. 72-81, 2016.

[12] Hua M D , Hamel T , Morin P , et al, "Introduction to feedback control of underactuated VTOLvehicles: A review of basic control design ideas and principles" . *IEEE Control Systems*, , vol. 33, no. 1)pp. 61-75. 2013.

[13] Voos H . "Nonlinear control of a quadrotor micro-UAV using feedback-linearization," *IEEE International Conference on Mechatronics*, 2009.

[14] Kamel M , Alexis K , Achtelik M , et al, "Fast Nonlinear Model Predictive Control for Multicopter Attitude Tracking on SO(3)," *2015 IEEE Conference on. Control Applications (CCA)*, 2015.

[15] KAMEL M, VERLING S, ELKHATIB O, et al, "The Voliro Omnidirectional Hexacopter: An Agile and Maneuverable Tiltable-Rotor Aerial Vehicle," *IEEE Robotics & Automation Magazine*, vol. 1,no. 1, 2018.

[16] Ryll M , Bicego D , Franchi A , "Modeling and control of FAST-Hex: A fully-actuated by synchronized-tilting hexarotor," *2016 IEEE/RSJ International Conference on Intelligent Robots and Systems (IROS)*, 2016.

[17] Bouabdallah S , Noth, André, Siegwart R, "PID vs LQ control techniques applied to an indoor micro quadrotor," *IEEE/RSJ International Conference on Intelligent Robots & Systems*, 2004.

[18] JOHANSEN T A, FOSSEN T I, "Control allocation—A survey," *Automatica*, vol.49, no.5, pp.1087-1103, 2013.

[19]ZENG Xiaoyong, PENG Hui1, "Modeling and attitude control for a quad-rotor aircraft," *Journal of Central South University (Science and Technology)* , vol. 44, no. 9, pp. 3693-3700, 2013.